X-701-69-172
TASK IIB
PREPRINT

SPACECRAFT CHARGE BUILD-UP ANALYSIS

A REPORT COVERING TASK IIB EFFORT
UNDER THE STUDY OF

NASA EVALUATION WITH MODELS OF OPTIMIZED NUCLEAR SPACECRAFT (NEW MOONS)

Wm. S. West, J. V. Gore, M. A. Kasha and Herbert W. Bilsky

APRIL 1969

GSFC
GODDARD SPACE FLIGHT CENTER
GREENBELT, MARYLAND

X-701-69-172
TASK IIB

SPACECRAFT CHARGE BUILD-UP ANALYSIS

A Report Covering Task IIB Effort Under The Study

NASA Evaluation With Models Of Optimized Nuclear Spacecraft
(NEW MOONS)

Wm. S. West, Technical Officer
Goddard Space Flight Center
Greenbelt, Maryland

J. V. Gore and M. A. Kasha
RCA Research Laboratories
Montreal, Canada

Herbert W. Bilsky
RCA
Astro-Electronics Division
Defense Electronic Products
Princeton, New Jersey

April 1969

GODDARD SPACE FLIGHT CENTER
Greenbelt, Maryland

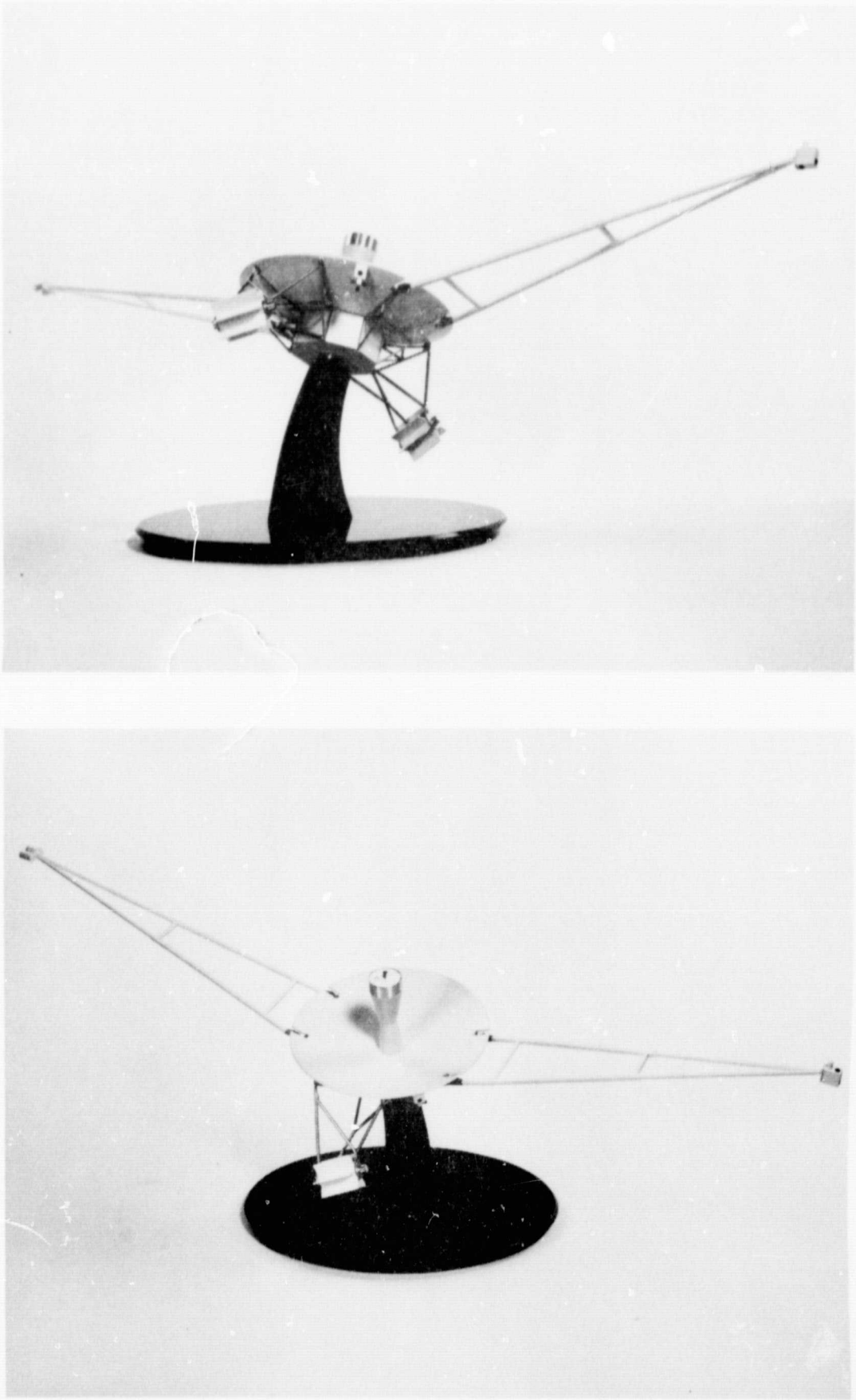

Frontispiece A—Two Views of a Model of the Galactic Jupiter Probe which served as the "Reference Design" for this Task

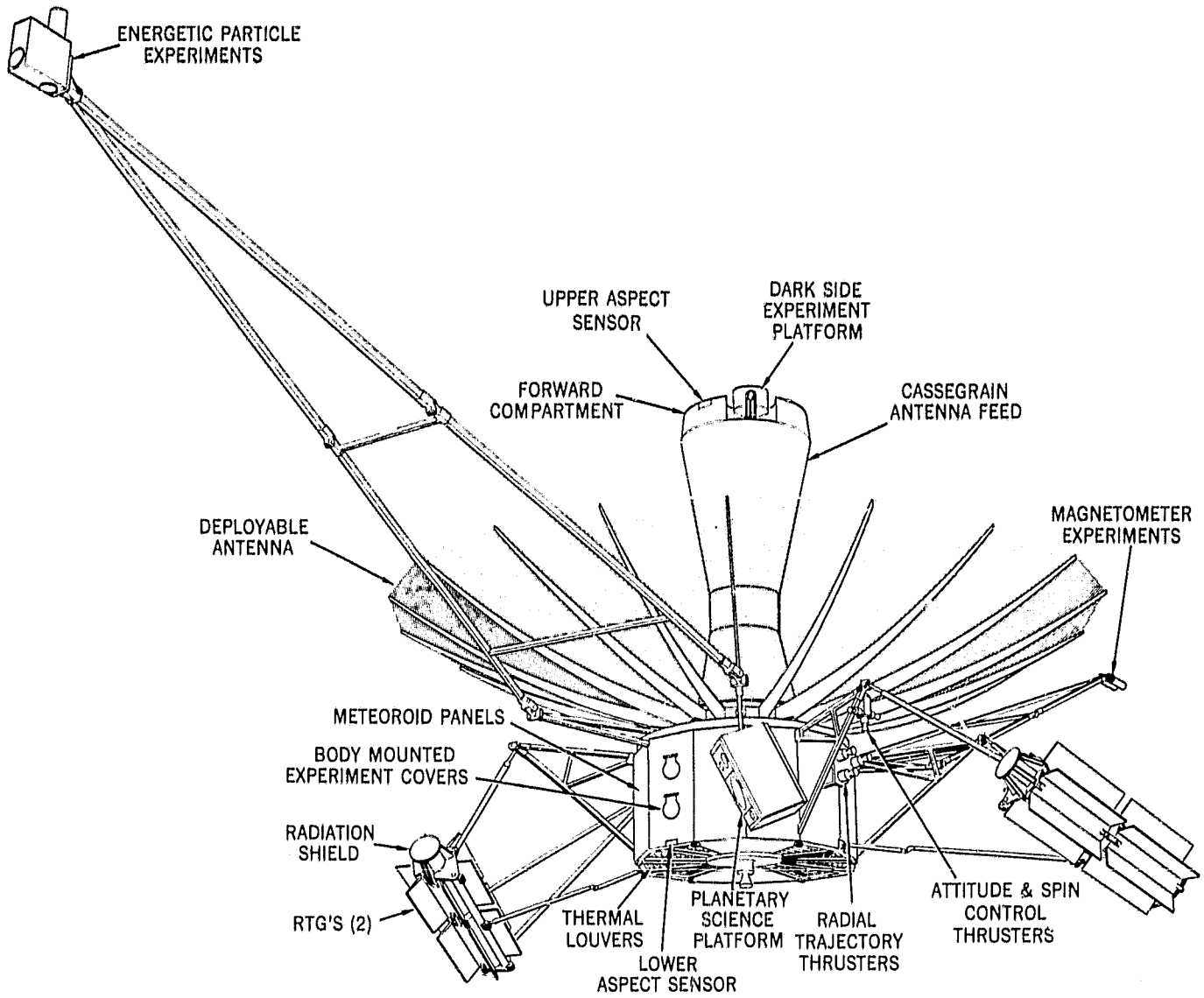

Frontispiece B–Outer Planets Explorer

SPACECRAFT CHARGE BUILD-UP ANALYSIS

A Report Covering Task IIB Effort Under The Study

NASA Evaluation With Models Of Optimized Nuclear Spacecraft (NEW MOONS)*

ABSTRACT

Spacecraft charge build-up mechanisms, as discussed in selected literature are reviewed. The practical aspects of spacecraft charge build-up are covered as they might be of concern to planners and designers of missions into deep space. Specific attention is directed toward the probable effects of small nuclear power supplies or RTG's on the general topic.

---

* NASA Evaluation With Models Of Optimized Nuclear Spacecraft (NEW MOONS) Contract NAS 5-10441, performed by RCA Astro-Electronics Division, Defense Electronic Products, Princeton, New Jersey for NASA Goddard Space Flight Center, Greenbelt, Maryland. RCA Research Laboratories, Montreal, Canada supported RCA Astro-Electronics Division for this Task.

ACKNOWLEDGMENT

Spacecraft Charge Build-Up Analysis

NEW MOONS Task IIB

PROGRAM GENERALLY:

In the course of conducting the studies of the NEW MOONS program valuable assistance has been provided by many people representing various organizations. It is considered appropriate to identify those whose contributions were most vital.

Fred Schulman, NASA Office of Advanced Research and Technology and Marcel Aucremann, NASA Office of Space Science and Applications both realized the necessity for the NEW MOONS studies and provided technical guidance and financial support throughout the program.

Daniel G. Mazur, Assistant Director for Technology and Rudolph A. Stampfl, Deputy Assistant Director both of Goddard Space Flight Center aided in program initiation.

RCA Astro-Electronics Division, the prime contractor, recognized the importance of the NEW MOONS program and has given its support and cooperation toward realizing the objectives of the program. Herbert Bilsky served in the capacity of RCA project manager and technically contributed to the program and provided aid in preparation and review of the manuscripts.

THIS TASK REPORT:

For this report J. V. Gore and M. A, Kasha of RCA Research Laboratories, Montreal, were the principal investigators and authors of the draft materials. F. J. Osborne, J. A. Nilson and T. W. Johnston of RCA Research Laboratories provided helpful comments and suggestions in the preparation of this report. K. Campe of Hittman Associates supplied the RTG radiation environment.

Goddard Space Flight Center personnel who have provided important technical information, review and comments include James Trainor, Emil W. Hymowitz, and Joseph H. Conn.

William S. West

William S. West, Technical Officer
Goddard Space Flight Center
Greenbelt, Maryland

PREFACE

BACKGROUND AND RELATED INFORMATION

Since the early 1960's, personnel of the Goddard Space Flight Center have been interested in deep-space missions to obtain information concerning the planets, Jupiter, Saturn, Uranus, Neptune and Pluto, as well as information concerning the interplanetary medium. Studies have been performed to establish the feasibility of such missions and various reports were written by Goddard personnel[1] and by others[1].

For almost as long as these missions have been considered, the engineers, scientists and managers at Goddard have realized the necessity for systems, independent of the Sun's energy, to supply the spacecraft electric power requirement. In general, Goddard studies have indicated that there is a weight advantage in using small nuclear power systems such as radioisotope fueled thermoelectric generators instead of presently available solar cells when missions go beyond 2.5 or 3 AU. Further, there are technological and practical uncertainties in projecting use of solar arrays in a range starting beyond 3-5 AU[2] whereas the use of small nuclear power supplies is technically and practically feasible. However, the use of small nuclear systems, while feasible, nevertheless presents technical questions. An in-house Goddard study[3] identified pertinent technological areas requiring study prior to the use of these nuclear generators on spacecraft designed for scientific deep space missions.[4] These areas were divided into the following numbered tasks:

---

[1] See X-701-69-170 Analysis of Selected Deep Space Missions.

[2] Technical uncertainties involve practical design questions arising from the use of very large solar array areas, their survival through meteroid belts and their system performance when operating at the low temperature and low illumination levels anticipated.

[3] See Task I, Reference 28.

[4] This study is referred to as NEW MOONS.

Task Number	Task Description — Title	Reference X Document
I	Analysis of Selected Deep-Space Missions	X-701-69-170
IIA	Subsystem Radiation Susceptibility Analysis of Deep-Space Missions	X-701-69-171
IIB	Spacecraft Charge Build-Up Analysis	X-701-69-172
III	Techniques for Achieving Magnetic Cleanliness	X-701-69-173
IV	Weight Minimization Analysis	X-701-69-174
V	Spacecraft Analysis and Design	X-701-69-175
VI	Spacecraft Test Documentation	X-701-69-176
VIIA	Planar RTG-Component Feasibility Study	X-701-69-177
VIIB	Planar RTG-Spacecraft Feasibility Study	X-701-69-178
VIII	RTG Interface Specification	X-701-69-179
~	Summary Report of NEW MOONS	X-701-69-190

Specific Rationale for Task IIB. E. C. Whipple, Jr's. Doctoral-Thesis, The Equilibrium Electric Potential of a Body in the Upper Atmosphere and in Interplanetary Space (Ref. 13) indicates that "a body in the upper atmosphere or in space will acquire an electric charge, or potential, which must be known ... to assess the behavior of certain experiments on satellites" (pg. iii) and on pgs. 57 and 58 states "... 3. Radioactivity. Radioactive material in a body in space constitutes a charging mechanism .... Satellites sometimes carry quantities of radioactive material in conjunction with certain types of experiments, or as a power source. Such sources are normally well shielded but should still be considered as potential charging mechanisms. Clearly, each such source must be evaluated individually."

The Task I, missions analysis report indicates the necessity for radioisotope-fueled thermoelectric generators (RTG's) for the mission into deep space.

This Task, Task IIB, therefore examines briefly the literature and current project plans and postulates the spacecraft potential that might be expected by the Galactic Jupiter Probe or Outer Planet Explorer. The variation in the naturally occurring discharging mechanisms is also considered.

A contract[5] was established for further study of these areas. This study was entitled NASA Evaluation With Models Of Optimized Nuclear Spacecraft (NEW MOONS). During the execution of the NEW MOONS Technology Study, Goddard was assigned the task of conducting a Phase A study covering a Galactic Jupiter Probe[6]. These two study efforts, Galactic Jupiter Probe and NEW MOONS, were directed to provide the maximum practical benefit to each other. In general, the Galactic Jupiter Probe was considered as a "base line spacecraft and mission" or a "reference design" during the NEW MOONS Technology Study. On the other hand, the Galactic Jupiter Probe Study team made use of the technology and data as developed by the NEW MOONS Study in areas of missions analysis, shielding, aerospace nuclear safety, thermal and structural analysis and other related areas.

As the NEW MOONS contract was being concluded, the scope of Galactic Jupiter Probe project was broadened and adopted the name Outer Planets Explorer (OPE)[7]. The Outer Planet Explorer is considered for a generally more ambitious program than the original Galactic Jupiter Probe, in that the OPE is intended for a family of single and multiple planet missions.

The OPE, as presently visualized, encompasses spacecraft in the 1100-1400 pound class whereas the GJP "reference design-spacecraft" for the NEW MOONS Study was 500-600 pounds. This is a significant practical difference from a flight project viewpoint; however, the technology and techniques of NEW MOONS are generally applicable. Specific numeric values will be different when solutions are developed, but the techniques and rationale indicated in the NEW MOONS reports are applicable to the general problem of integrating and using small nuclear power systems on a scientific spacecraft designed for deep space missions.

APPLICABILITY TO OTHER PROGRAMS

The NEW MOONS technology and techniques reported may have applicability or some relevancy to additional space missions that may in the future use nuclear systems such as planetary landers and rovers as well as applications spacecraft.

[5]NAS 5-10441 RCA Astro-Electronics Division, Princeton, N. J.

[6]See Task I, References 1 and 2. See Frontispiece A.

[7]See Task I, Reference 37. See Frontispiece B.

CONTENTS

CONTENTS (Continued)

LIST OF ILLUSTRATIONS

LIST OF ILLUSTRATIONS (Continued)

LIST OF TABLES

GLOSSARY OF SYMBOLS USED IN TASK IIB

A	Correction factor such that $1 \leq A \leq 2$, due to magnetic field
B	Magnetic Field
B_o	Equatorial Magnetic Field of Jupiter
E	Energy level
E_i	Ion energy
e	Electron charge
$f(E_i)$	Ion energy spectrum
I_e	Electron current
I_i	Ion current
i_{ph}	Photoelectric current density
i_r	Total current density to the body by one component
k	Boltzmann's constant
M	Ion mass
m	Electron mass
n	Electron (and ion) density
n_e	Electron density
n_i	Ion density
R_e	Earth radii
R_j	Jupiter radii
r	Radius of the sphere

r_s	Distance from sun
T_e	Electron temperature
T_i	Ion temperature
V_f	Floating potential
V_o	Spacecraft velocity
V_o'	Spacecraft velocity in nonrotating frame
$\delta(E_i)$	Secondary electron yield
$\delta_{i,e}$	Secondary emission coefficient for ions or electrons
ϕ	Potential
ϕ_i	Ion thermal flux
ΩR_j	Particle velocity relative to spacecraft

SPACECRAFT CHARGE BUILD-UP ANALYSIS

A Report Covering Task IIB Effort Under The Study

NASA Evaluation With Models Of Optimized Nuclear Spacecraft
(NEW MOONS)

SECTION I

INTRODUCTION AND SUMMARY

A. INTRODUCTION

The purpose of the analysis performed in Task IIB was to determine the extent of charge build-up to be anticipated for a deep-space spacecraft due to the RTG and space environments and the effect that this estimated charge build-up would have on the spacecraft subsystems. For this Task the GALACTIC JUPITER PROBE (GJP) spacecraft described in the Task V report and in the Galactic Jupiter Probe Report* has been selected as the baseline configuration. A photograph of an 1/18 scale model of this spacecraft is shown in Figure 1. The analytical techniques used in this report are somewhat independent of the baseline spacecraft configuration selected and the techniques are generally applicable to any deep-space mission or spacecraft configuration. It will be shown that effects due to the RTG's are negligible in the cases studied; however, the effects due to the space environment, particularly with respect to experimental sensors, merit consideration. As the spacecraft travels along its flight path from Earth to the regions of Jupiter, and beyond it will be constantly bombarded by charged particles, principally electrons, positive ions, protons, and also photons, causing an accumulation of charge on the spacecraft. The rate of flow of positively and negatively charged particles to and from the surface of the spacecraft determines its equilibrium, or floating potential. Equilibrium potential is established when the total current entering or leaving the spacecraft is zero. In a plasma with an equal number of electrons and positive ions, at approximately the same particle temperature, the equilibrium potential of a conducting surface will be slightly negative. This results from a higher electron flux because of the higher electron velocity. If protons are present in much larger quantities, the result will be a positive equilibrium potential. Photoelectrons generated by the effect of sunlight on the spacecraft surface can also alter the floating potential, tending to make it more positive; secondary emission from bombarding electrons will have a similar effect.

*Galactic Jupiter Probe, Phase A Report, GSFC X701-67-566, November, 1967. The spacecraft weight is approximately 600 pounds and its 2 RTG's each contain approximately 1725 watts (thermal) of PuO_2 fuel.

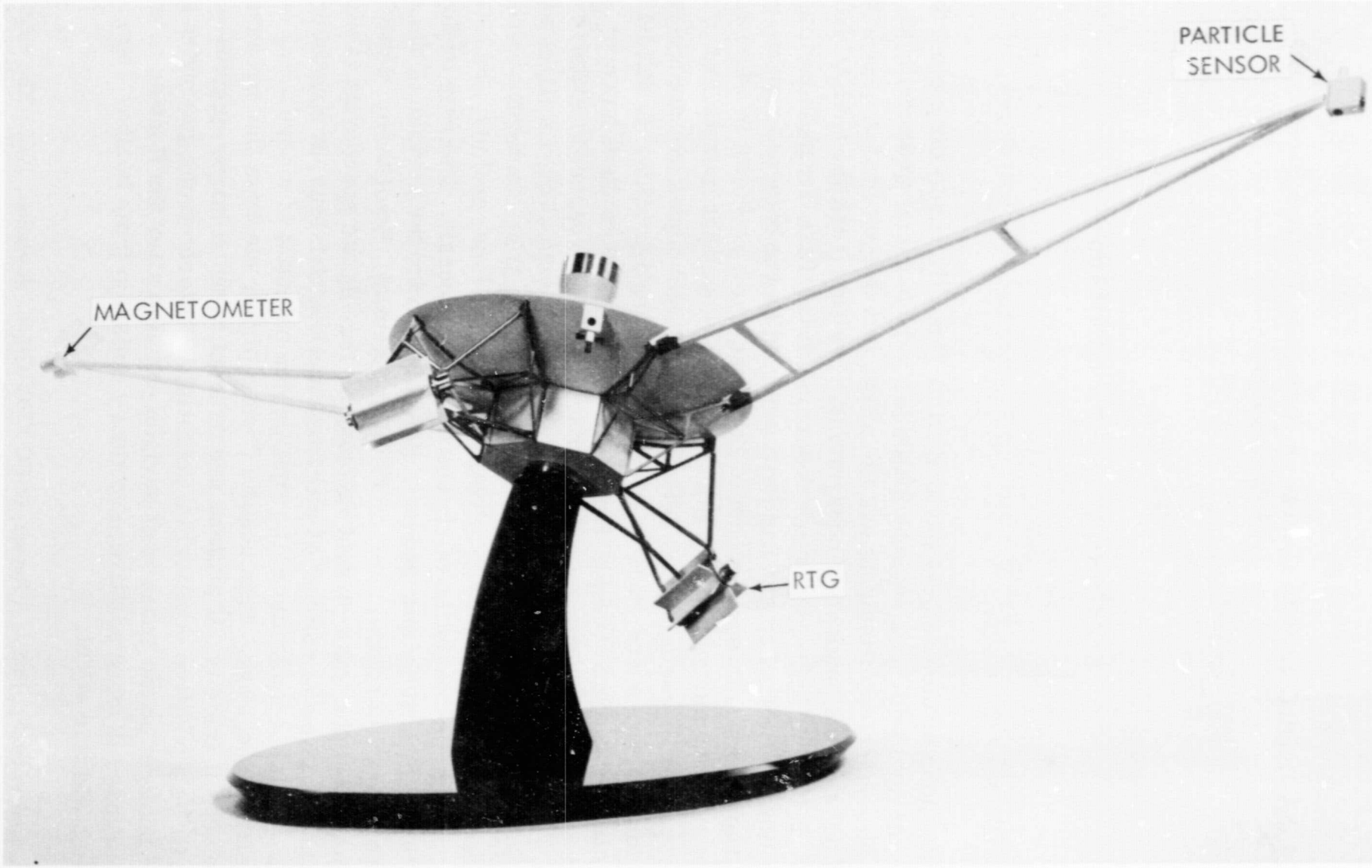

Figure 1. Model of the Galactic Jupiter Probe

In this analysis of spacecraft charge build-up, the sources of charge will be considered. These sources include the RTG's as well as natural environment. In evaluating the natural sources of charge build-up, the regions of near-Earth, interplanetary space, and near-Jupiter will be considered separately; the particle effects that are not limited to a particular region, such as photoemission and secondary-emission are also considered. The spacecraft potential resulting from these sources of charge build-up for various regions of space is estimated and possible measures for avoiding difficulties from charge build-up effects are recommended.

In the interplanetary space or regions beyond Jupiter, the charge-discharge mechanisms may be significantly altered from the models assumed in this report. If one postulates pockets of extremely low charged particle density, or "voids", then the charge build-up due to on-board RTG's may become relatively more significant than is indicated by the models used in this report.

Similarly, this report does not specifically cover the considerations associated with charged-particles originating outside of the solar system. This, too, may significantly alter the charge-discharge mechanism.

B. BACKGROUND

The subject of charge build-up on a body in space has been considered for some 25 years even prior to the advent of earth orbiting satellites. One of the first papers to discuss the subject of the equilibrium of electric charge appeared in 1937*. This paper treated positive ion and electron collection and photoemission. Other papers subsequently appeared extending and refining the analysis until 1956 when Lehnert† applied analysis to a postulated earth orbiter. A few years later Sputnik III actually measured spacecraft charge and indicated a negative potential varying from -2 volts to -7 volts with altitude and with day-night conditions. Other papers appeared later continuing the process of analytical refinement but with the addition of measurements provided from earth orbiters and rocket flights. It can be seen that this subject has received considerable study over the years, and is in a continuing state of reevaluation as new measurements are made and as new theories are proposed.

It is interesting to note the developing picture of the Earth's magnetic field, which is associated with the subject of charge build-up, brought about as a result of space-age observations. This is dramatically illustrated in Figure 2A and B, the latter representing today's view.

*B. Jung, Astron. Nach., 263, 426 (1937).

†B. Lehnert, Tellus, 8, 408 (1956).

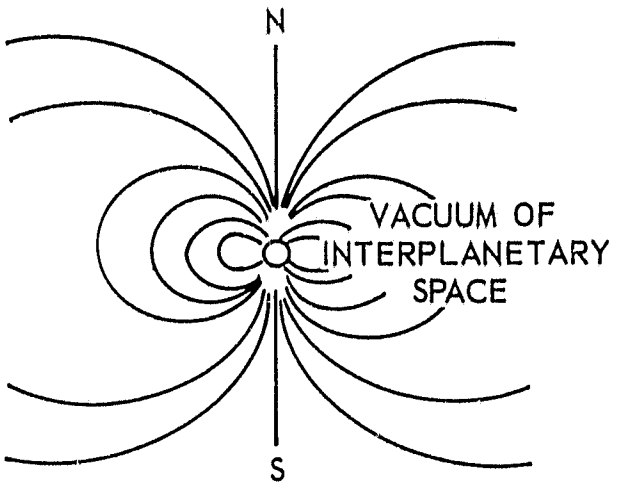

A. Simple dipole model of Earth's magnetic field, representing earlier understanding.

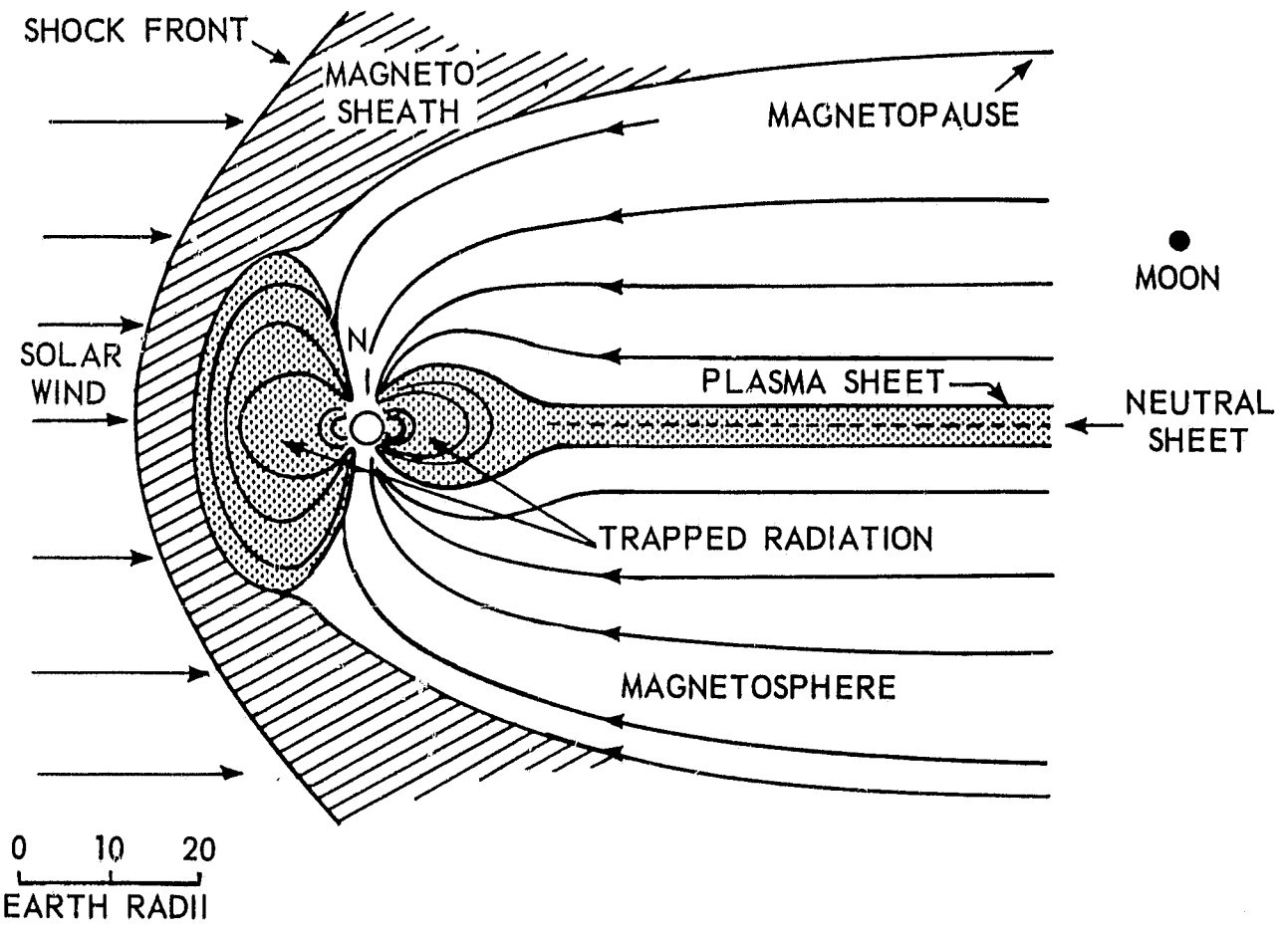

B. "Doughnut and tail" model of Earth's magnetic field, representing present concepts after a decade of spacecraft observations. Dot marked "Moon" indicates relative distance at which the Moon's orbit intersects plane of view. View plane contains Sun-Earth line and geomagnetic axis.

Figure 2. Earth's Magnetic Field*

*Physics of the Earth in Space, A Report of a Study by the Space Science Board, Woods Hole, Massachusetts, National Academy of Science, October 1968.

Study has indicated that RTG's will be required on deep-space missions and this Task is to consider their impact on the charge build-up problem. A preliminary search of the literature has not indicated its study previously.

C. SUMMARY

This report discusses the mechanism of spacecraft charge build-up, and the resulting equilibrium floating potential on a selected deep-space spacecraft, Figure 1, in the various environments to be encountered. The parameters of the relevant regions of space are presented. Where experimental data are available, the representative values, and the range of values, have been indicated. Where no datum exist, the values of the parameters are based on models from several authors. As a result data on the near-Jupiter region are, therefore, speculative, and wide excursions from the given numbers are probable. Similarly, data for the region of interplanetary space beyond Jupiter to 10 AU are speculative, although extrapolation for this region based on data in the 1 to 1.5 AU area were used. The regions of space beyond 10 AU and out-of-the-ecliptic plane were not studied.*

Approximate equations for the equilibrium floating potential of a spherical body (used as a model for the spacecraft) have been developed from equations for the collection of charge from the major sources as a function of body potential. The major sources of charge are: (1) electrons and ions from the thermal plasmas; (2) high energy particles; (3) secondaries produced as a result of particle impact; and (4) photoelectrons. In addition to these major sources, RTG's contribution to the charging mechanism has been considered. Near Earth, the flux of electrons and protons is at least two orders of magnitude less than the thermal electron and photoelectron flux. In the region of Jupiter's proton radiation belt, however, there may be a large proton flux in addition to a low thermal-electron density, which will charge the spacecraft several tens of volts positive. The RTG units, it has been found, do not contribute significantly to charge build-up at any time during the mission to Jupiter and even to a distance of 10 AU. Extrapolation relative to the importance of RTG's in the charge build-up mechanism for distances beyond 10 AU and out-of-the-ecliptic plane, were not made in this study.

The spacecraft equilibrium potential for each region through which the spacecraft passes is shown in Table 1. These values are given for average condition of solar activity. The potential for near-Earth and near-Jupiter regions

*For a description of the uncertainties of deep-space and out-of-the-ecliptic regions see "Physics of the Earth in Space, A Report of a Study by the Space Science Board", Woods Hole, Mass., National Academy of Science, October 1968.

Table 1

Summary of Regions Considered

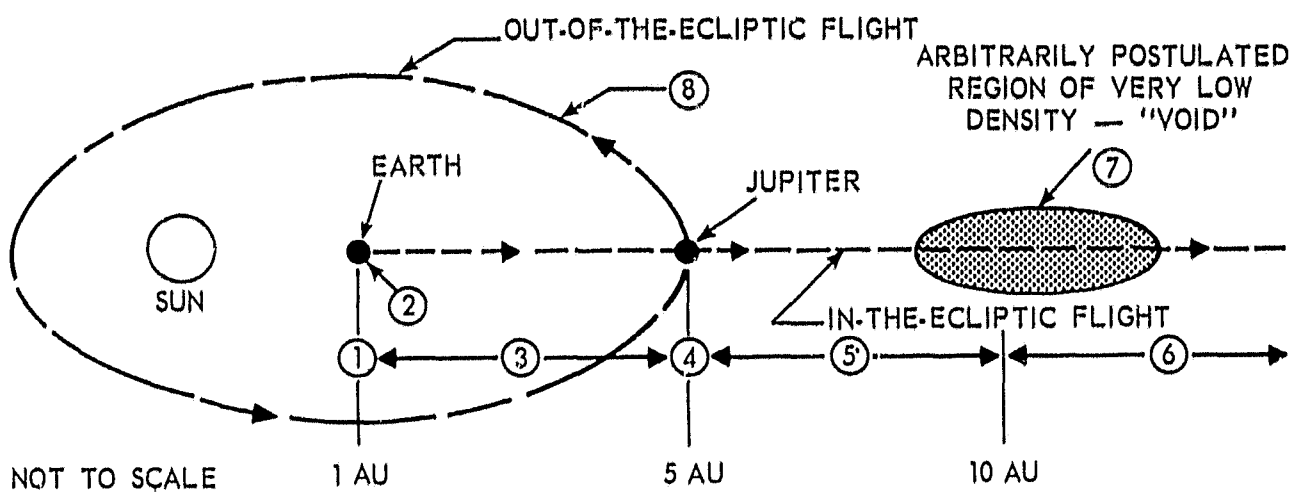

Region	Distance From Sun	Spacecraft Potential - Average Condition of Solar Activity	Remarks
1. Near-Earth	1 AU	3.5 Volts at 9 R_e See Figure 9 for Variation of Potential with R_e	
2. Earth's Magnetosheath	~1 AU	1.6 Volts	
3. Interplanetary	1 AU - 5 AU	3.4 Volts	
4. Near-Jupiter	5 AU	26 Volts at 9 R_j See Table 7 for Variation of Potential with R_j	Jupiter Model (Ref. 10)
5. Interplanetary	5 AU - 10 AU	3.4 Volts	Environment Uncertain, but Extrapolated Based on 1 - 1.5 AU Data
6. Interplanetary	Beyond 10 AU	—	Not Examined in this Task
7. "Void"	—	—	
8. Out-of-the-Ecliptic	—	—	

vary with the distance from the planet, but the value in the Table is shown only for 9 planetary radii. The value given for the Interplanetary region will not vary as long as the charge particle density varies as $\frac{1}{r_s^2}$ and the particle velocity and temperature remain constant. For this report it is assumed that these conditions would be present out to the region of approximately 10 AU.

The influence of the floating potential on possible experiments is briefly discussed in Section V. In summary it can be stated that experiments designed to measure the thermal electrons or ions will be adversely affected by the spacecraft potential. It is therefore necessary for these experiments to have a collector with a large enough dynamic voltage range so that it may sweep the sensor through and appreciably beyond the plasma potential. The effects of the electron sheath around the spacecraft, created by a charged spacecraft must also be considered when interpreting the data. Experiments measuring high-energy particles (i.e., particle energy (eV) >> spacecraft potential) will not be affected appreciably by the spacecraft potential.

SECTION II

ANALYSIS OF THE CHARGED-PARTICLE ENVIRONMENT

A. CHARGE BUILD-UP MECHANISM — BRIEF DESCRIPTION

A spacecraft on an interplanetary trajectory is constantly exposed to charged and uncharged particles and to photons. When an encounter occurs, a charge transfer to or from the body will take place. This mechanism of charge transfer can be classified as charge collection or charge emission. The latter consists of processes such as photoemission, secondary emission (due to impingement of energetic particles on the body) thermal emission and field emission. Because of the presence of RTG's on the spacecraft another charge emission mechanism is present due to the radioactive materials. The most important processes for the region of space considered for this Task are the collection of environmental electrons and ions and photoemission and secondary emission. These mechanisms, as well as RTG emission, are treated in this report. There are other less important charging mechanisms, which are not treated here, such as cosmic rays, collisions with dust grains and the previously mentioned thermal emission and field emission.

A distinction should be made in the charge build-up process between energetic particles and lower energy (thermal) particles in that the latter are influenced by the spacecraft charge present whereas the former are essentially independent of spacecraft charge. It is also noted that the production of electrons by photoemission and secondary emission is dependent on the target material and perhaps even the "cleanliness" of the material (presence of oxides). Throughout this report aluminum is assumed to be the exposed material except for the RTG's where beryllium is assumed.

In summary, then, the rate at which charge build-up proceeds is dependent on the charging or discharging mechanism, the spacecraft materials and the net charge already present.

B. THE SPACE ENVIRONMENT

The principal energy source of concern in the solar system is the Sun. The Sun is coupled to the environment of the planets by way of the interplanetary medium. The Sun's varying input to the interplanetary medium and its impact on solar wave particle radiation and plasma flow is of primary concern. This naturally occurring environment and the environment associated with RTG's are treated in this Section. It is recognized that particles originating outside of the

solar system may be of increasing importance to the charge build-up processes as the spacecraft distance from the Sun increases; but, these sources are not considered in this report. Also areas of extremely low charged particle density or "voids" have not been postulated or studied in this report.

In evaluating the sources of charge build-up, the regions of near-Earth, near-Jupiter, and interplanetary space are considered separately as was done in Radiation Susceptibility Analysis, Task IIA. In this discussion, however, the near-Earth and near-Jupiter regions are each divided into two parts: (1) the magnetosphere, which is that region near the Earth where the effect of the Earth's magnetic field on high-energy particles is predominant, and (2) the magnetosheath, which is the transition region between the magnetosphere and interplanetary space, see Figure 2. The inner boundary of the magnetosheath is called the magnetopause and the outer boundary the bow shock wave. In this outer boundary region, the particles emanating from the Sun, commonly referred to as the Solar Wind, are deflected from their normal paths by the magnetic field of Earth. It is assumed that the region near-Jupiter follows the same pattern as the near-Earth region. Since little is known about the environment near-Jupiter, the available data on the near-Earth particle environment provide useful background information for assuming the environment surrounding Jupiter although wide variations between these assumptions and reality may exist.

1. Earth's Magnetosphere

In this region, particles in two different categories are considered. The first category includes the thermal electrons and positive ions that have relatively low energies and, therefore, insignificant penetrating capability. The second category includes the high-energy electrons and protons trapped in the Van Allen belt whose radiation-damage-producing capabilities have been discussed in Task IIA.

The density of thermal electrons in the magnetosphere decreases rapidly with increasing altitude and is also strongly dependent on solar activity, which varies periodically (about 11 year cycle) between highly disturbed and relatively quiet conditions. The two curves in Figure 3 show the predicted variations in electron density up to an altitude of 8 R_e (Earth radii) for maximum and minimum conditions of solar activity. These curves are based on recent data published by Gendrin, Haydon, and Lucas (Refs. 1 and 2). It should be noted that throughout this report distances referred to in terms of planetary radii assumes it is measured from the center of the planet.

The temperature of the thermal electrons is less clearly defined; besides increasing with altitude and being affected by solar activity, it is also subject to considerable variation between daytime and nighttime. The matched curves in

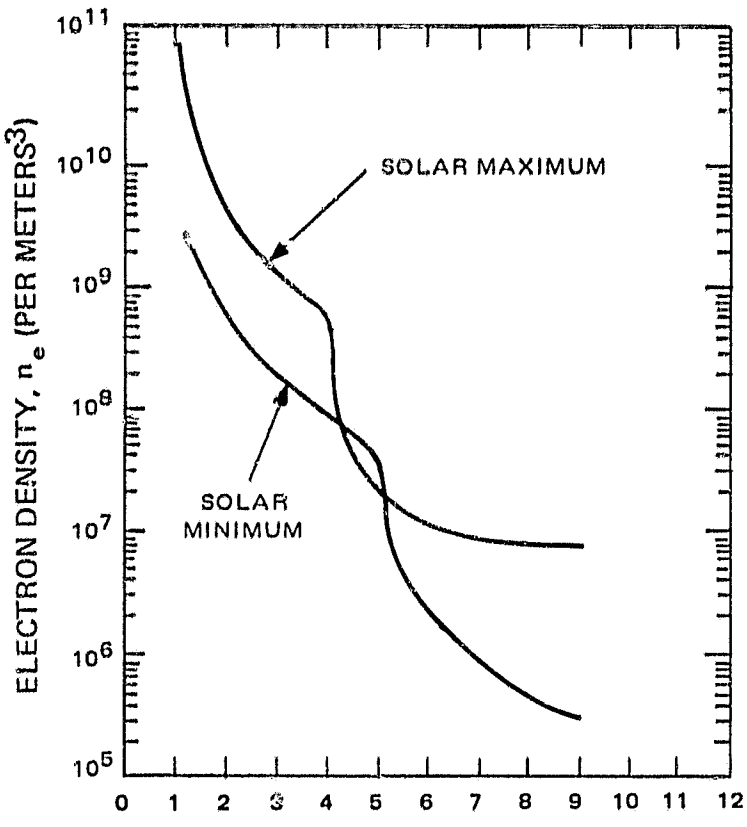

Figure 3. Electron Density in the Magnetosphere (Based on Ref. 1 and 2)

Figure 4 relating electron temperature to altitude show the anticipated variation between daytime and nighttime, based on data from Al'pert, Serbu, Maier (Refs. 3 and 4). At 1000 km the values of 1500°K and 3050°K are appropriate for nighttime and daytime, respectively.

The upper curve in Figure 4 (maximum solar activity) in the region above 2.6 R_e is given by Al'pert (Ref. 3) who quotes recent OGO-A data. Serbu and Maier (Ref. 4) have reported measurements of the electron temperature at radii from 2 to 9 R_e and found a temperature generally less than 22,000°K and a dependence on altitude of the form

$$T_e \propto R_e^{\,b} \tag{1}$$

where b is a number between 1.3 and 3.9. If b is taken arbitrarily as equal to 2.4 for disturbed conditions of solar activity, then the daytime temperature of 3050°K at 1000 km is in harmony with Al'pert's values above 2.6 R_e. In a similar manner, if b is assumed equal to 1.9 for nighttime conditions the temperature at 1000 km is in line with the low temperature data of Serbu and Maier.

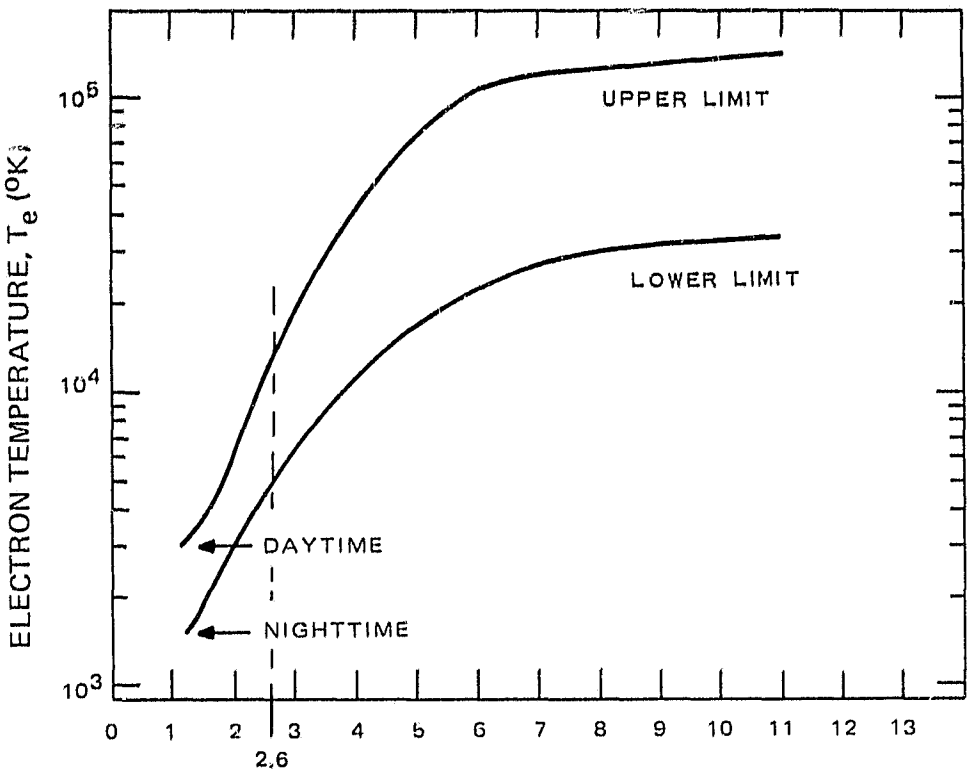

Figure 4. Electron Temperature in the Magnetosphere (Based on Ref. 3 and 4)

The two curves of Figure 4 obtained in this manner are, therefore, considered approximate upper and lower limits of electron temperature in the magnetosphere.

Calculations of the omnidirectional thermal particle flux in the magnetosphere from the data provided in Figures 3 and 4 are based on the expressions:

$$\varphi_e = n_e \left(\frac{8\,k\,T_e}{\pi\,m} \right)^{1/2} \tag{2}$$

and

$$\varphi_i = n_i \left(\frac{8\,k\,T_i}{\pi\,M} \right)^{1/2} \tag{3}$$

where

φ_e is electron thermal flux

φ_i is ion thermal flux

k is Boltzmann's constant

n_e is electron density

n_i is ion density

T_e is electron temperature

T_i is ion temperature

m is electron mass

M is ion mass

As these expressions indicate, the thermal particle flux is simply the product of the particle density and average velocity, assuming a Maxwellian distribution. The curves in Figure 5 showing the variation in particle flux with geocentric radius are derived from Figures 3 and 4 with the aid of these equations. The horizontal line indicating photoelectric current density, i_{ph}, has been included in Figure 5 for comparison purposes, which will be discussed later in Section III of this Report.

In addition to the thermal particles in the magnetosphere, the high-energy electrons and protons trapped in the Van Allen belt may also contribute to the charge build-up process. The curves in Figures 6 and 7 showing trapped electron and proton flux as a function of geocentric radius were taken from NASA and other publications (Refs. 5 and 6). Information of the same nature was used in estimating the radiation dose resulting from passage of the spacecraft through the Van Allen belt, as discussed in Task IIA. In Figure 6, the two curves show how the trapped electron flux above two different energy levels varies with geocentric radius. Figure 7 provides trapped proton flux data in a similar form. These data are based on averages for a 24-hour period near the plane of Earth's geomagnetic equator. The scale pertaining to current, included in Figures 6 and 7, pertains to a later discussion given in Section III of this report.

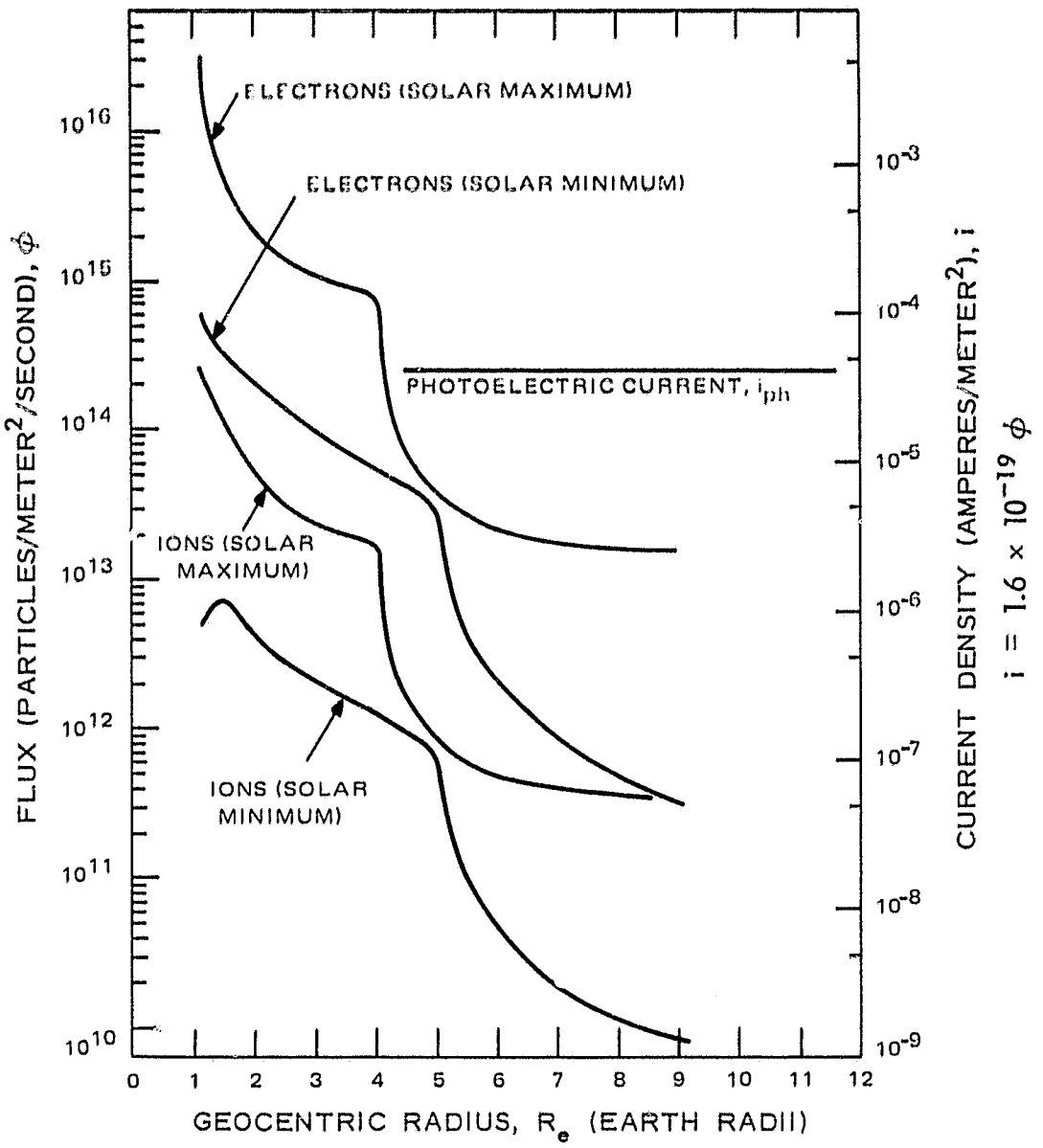

Figure 5. Thermal Electron and Ion Fluxes in the Magnetosphere

2. Earth's Magnetosheath

In the transition region between the magnetosphere and interplanetary space, the spacecraft will pass through the magnetosheath. The spacecraft will penetrate the magnetosheath presumably near the dawn meridian. Estimates of the charged particle population in this region are available in the literature. The data in Table 2 are based on the model by Spreiter et al. (Ref. 7), which appears to be in reasonable agreement with actual measurements. The charged particles of principal importance in this region are those particles that constitute the Solar Wind. Since the number and energy of charged particles depend on the degree of solar activity, Table 2 provide data for minimum, average, and maximum anticipated conditions.

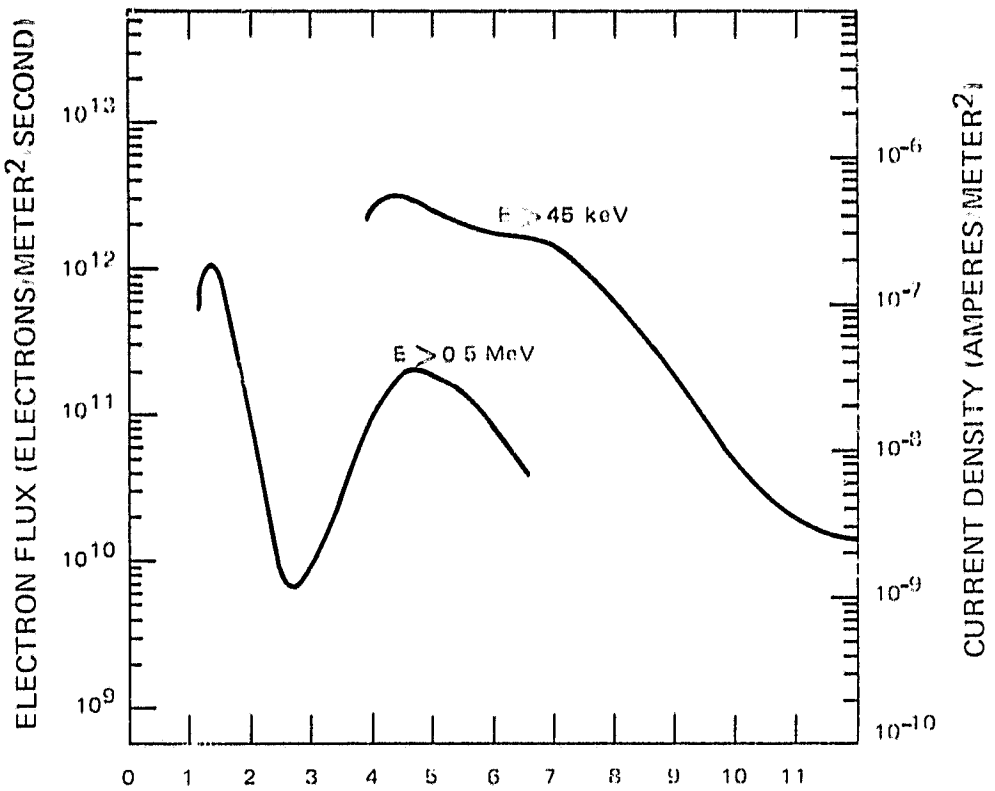

Figure 6. High-Energy Electron Flux in the Magnetosphere (Ref. 5)

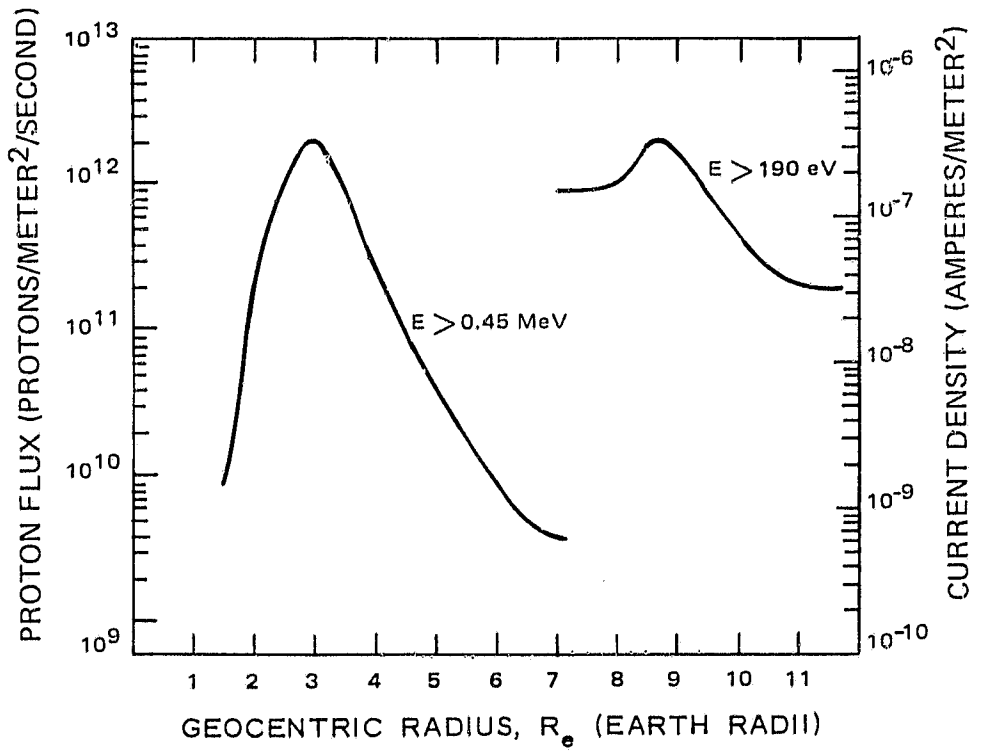

Figure 7. High-Energy Ion Flux in the Magnetosphere (Ref. 5 and 6)

Table 2

Parameters in the Earth's Magnetosheath and in Interplanetary Space at 1 AU

Parameter	Earth's Magnetosheath (Region 2, see Table 1)			Interplanetary Space (At 1 AU within Region 3)		
	Min.	Avg.	Max.	Min.	Avg.	Max.
Density, n_e (in Particles/m^3)	5×10^6	10^7	2.5×10^7	2×10^6	4×10^6	10^7
$T_e = T_i$ (in °K)	4.5×10^5	7.5×10^5	1.5×10^6	3×10^4	5×10^4	10^5
Flow Velocity (in meters/second)	2.25×10^5	3×10^5	4.5×10^5	3.0×10^5	4×10^5	6.0×10^5

3. Interplanetary Space

The data for the charged particles in interplanetary space, also included in Table 2, are for the same conditions of solar activity and are given for the region just beyond the magnetosheath at a distance of 1 AU, see region 2 of Table 1. At greater distances from Earth, the density is assumed to decrease as $1/r_s^2$ where r_s is the distance from the Sun. The velocity and temperature are assumed to be constant to the orbit of Jupiter and out to a distance of 10 AU, see region 3 and 5 of Table 1.

4. Near-Jupiter Environment — Magnetosphere and Magnetosheath

The charged-particle environment in the region near Jupiter is the subject of considerable speculation. The available data are based on observations of radio emissions from the direction of Jupiter at decimeter and decameter wavelengths. Such data provides a rough approximation of the probable extent of the magnetosphere surrounding Jupiter (Ref. 8).

Values quoted for the magnetic field of Jupiter, based on probable mechanisms for radio emission, are from 10 to 30 gauss on the planet's equator. Based on these values and the assumption that the Jupiter magnetopause is located at the position where the kinetic plasma pressure would equal the magnetic pressure, the location of the magnetopause of Jupiter is estimated to be between 60 and 90 R_j (Jupiter radii). The spacecraft trajectory, discussed in Task I, "Mission Analysis" should, therefore, be well inside the Jupiter magnetosphere.

The plasma density of the near-Jupiter region, which will greatly affect the charging of the spacecraft, is unknown. Ellis (Ref. 9) has postulated a mechanism for the decameter radio emission from Jupiter and has developed a model for the plasma density in the ionosphere and out to 2 R_j. In a paper that discusses the planet's rotational effects on the distribution of thermal plasma in the magnetosphere of Jupiter, D. B. Melrose (Ref. 20) concluded that in the range of 2.5 to about 8 R_j the thermal plasma density decreases as $1/R_j^4$. Beyond 8 R_j the plasma breaks into bunches. For the purpose of calculation it is assumed that the plasma density decreases as $1/R_j^4$ beyond 8 R_j and the density at 2 R_j is 10^9 electrons/meter^3 (Ref. 10).

Table 3 gives values for parameters at several planetary radii from Jupiter. The minimum and maximum electron densities are taken simply as 1/5 and 5 times the average density. Electron and ion temperatures are assumed to be 50,000°K.

The column ΩR_j is included, for if the magnetosphere of Jupiter corotates with the planet (Ref. 9) the spacecraft velocity relative to the rotating plasma will be $(\vec{\Omega} \times \vec{R}_j) + \vec{V}_o'$ where V_o' is the velocity of the spacecraft in a non-rotating frame.

The magnetic field has simply been quoted as B_o/R_j^3 where B_o is the equatorial magnetic field of Jupiter and is taken as 1.5×10^{-3} Teslas.* Magnetic field values for various R_j distances are given in Table 3.

High-energy electrons and protons are also assumed to be part of the near-Jupiter environment along with the thermal particles. These high-energy particles, presumably trapped in the magnetic field surrounding Jupiter, may contribute significantly to radiation damage in spacecraft components, as outlined in Task IIA where the various factors involved in estimating particle population and energy distribution are treated in detail. The principal source of such information used for this Task is a recent report by Eggan (Ref. 10). Eggan's report, however, only provides such data over relatively limited energy ranges, 0.1 to 4 MeV for protons and 5 to 100 MeV for electrons. Using Earth's Van Allen belt as a model, estimates were prepared of the trapped protons above 4 MeV and trapped electrons below 5 MeV, since particles in these energy ranges are of major importance in assessing radiation damage effects, (Ref. Task IIA). In considering charge build-up effects, however, the same assumptions with respect to particle population do not correspond to the possible worst-case condition, i.e., maximum charge build-up. For this reason calculations of the anticipated

*1 Tesla = 1 Weber/meter^2 = 10^4 Gauss

Table 3

Near-Jupiter Environment Parameters

Radius R_j (Jupiter Radii)	Electron Density Range	Electron Density n_e (part./m^3)	Electron Temperature T_e (°K)	Photo-electric Current i_{ph} (amp/m^2)	Particle* Velocity Relative to S/C ΩR_j (m/sec)	Magnetic Field† B (Teslas)
8	Min. Av. Max.	7.8×10^5 3.9×10^6 2.0×10^7	50,000	1.5×10^{-6}	1.0×10^5	2.9×10^{-6}
9	Min. Av. Max.	4.9×10^5 2.4×10^6 1.2×10^7	50,000	1.5×10^{-6}	1.6×10^5	2.1×10^{-6}
10	Min. Av. Max.	3.2×10^5 1.6×10^6 8.0×10^6	50,000	1.5×10^{-6}	1.27×10^5	1.5×10^{-6}
15	Min. Av. Max.	6.2×10^4 3.2×10^5 1.6×10^6	50,000	1.5×10^{-6}	1.9×10^5	4.4×10^{-7}
20	Min. Av. Max.	2.0×10^4 1.0×10^5 5.0×10^5	50,000	1.5×10^{-6}	2.5×10^5	1.9×10^{-7}
30	Min. Av. Max.	4.0×10^3 2.0×10^4 9.9×10^4	50,000	1.5×10^{-6}	3.8×10^5	5.6×10^{-8}
50	Min. Av. Max.	5.1×10^2 2.6×10^3 1.3×10^4	50,000	1.5×10^{-6}	6.3×10^5	1.2×10^{-8}

*Ω for Jupiter is 1.76×10^{-4}/sec.

† B_o at $R = 1R_j$ is 1.50×10^{-3} Teslas
(1 Tesla = 1 Wb/m^2 = 10^4 gauss

charge build-up in the region near Jupiter disregard particles in energy ranges outside those given by Eggan. Under such circumstances an important source of charge build-up will be the protons in the 0.1 to 4 MeV energy range. At 9 R_j, Eggan's data indicate that the trapped proton flux will be 10^{13} protons/meter^2/sec, corresponding to a current density of 1.6×10^{-6} amps/meter^2. As will be shown in Section III, this current constitutes a possible major source of charge. However, if the extrapolation process used in evaluating radiation damage effects from electrons in the range below 5 MeV is valid, then the effect of the trapped protons in producing charge build-up will be greatly reduced.

C. OTHER CHARGING SOURCES (EXCLUDING RTG's)*

1. Photoemission

Light from the Sun, especially in the UV part of the spectrum, will induce emission of electrons from the spacecraft in sufficient quantity to affect significantly its potential. The emission of electrons from a surface is dependent on the material and on the spectrum of the incident light. In the absence of other charging effects, the resulting potential would be positive. For a body at a negative potential all the emitted electrons will escape and the current is independent of the potential. To determine the photoelectric current from a body at a positive potential, it is necessary to know the energy spectrum of the emitted electrons. For conditions where the Debye shielding length is much larger than the spacecraft the number of electrons escaping will simply be those with energies greater than the potential difference between the spacecraft and the ambient plasma. If the body is large, then the escape of electrons is dependent on the angular distribution of the emitted electrons and the body geometry. Since, in interplanetary space, and at large Earth radii in the magnetosphere, the Debye length is large and as a typical deep-space spacecraft is a complex shape, the number of electrons escaping will be taken as those with an energy larger than the potential. There have been several measurements of the photoelectron current density at Earth (Ref. 11). An average value, and the value that will be used for calculation purposes, is 4×10^{-5} amperes/meter^2. In interplanetary space this value will decrease as $1/r_s^2$, where r_s is the distance from the Sun. The photoelectric current vs. retarding potential was determined by Hinteregger and Damon (Ref. 12). Fahleson (Ref. 11) states that the spectrum of photo-electrons is approximated by a Maxwellian distribution with a temperature T_{ph} equivalent to 1 eV.

*See paragraph D of this Section for discussion of RTG's.

2. Secondary Emission From High-Energy Particle Radiation

To evaluate the contribution to the current density to the spacecraft from high-energy radiation, it is necessary to consider the incident flux and the emission of secondary electrons it produces. The total current density to the body by one component (ions, plus sign; or electrons, minus sign) is:

$$i_r = \pm e \,(\text{incident flux})\,(1 \pm \delta_{i,e}) \qquad (4)$$

where $\delta_{i,e}$ is the secondary-emission coefficient for ions or electrons. For metals, the electron secondary emission for high-energy electron bombardment is not more than 1.7, and this value only over a small incident electron energy interval. The maximum secondary emission for proton bombardment for aluminum is 4 (Ref. 13).

To determine the secondary-emission current, Equation (5) should be evaluated

$$i_r = e \int_{E_i} f(E_i)\,[(1 + \delta(E_i)]\; d\,E_i\,, \qquad (5)$$

where:

$f\ (E_i)$ is the ion energy spectrum,

$\delta\ (E_i)$ is the secondary electron yield and,

E_i is the ion energy.

The secondary-electron yield function $\delta\ (E_i)$ is given by Whipple (Ref. 13) and representative ion energy spectra are given in Reference 14. For a negative spacecraft this integral is the total current density. For a positive spacecraft the energy spectrum of the secondary electrons must be taken into account in a similar way as the photoelectron spectrum.

D. RTG RADIATION ENVIRONMENT

(i.e., Particle environment directly attributable to the presence of RTG's that would not otherwise exist.)

Radiation emitted by the RTG units consists primarily of neutrons and gamma rays. Neither type of radiation will have a direct effect on the potential of the

spacecraft. Interaction of gamma photons with RTG materials and certain spacecraft materials produce electrons. Many of these will have sufficient energy to leave the spacecraft and will therefore tend to cause a positive spacecraft potential.

The electron emission rate was computed for a 75 watt(e) RTG.* The maximum gamma flux near the outside of the RTG is about 2.5×10^5 photons/cm^2 - sec, as computed by the ISOQAD shielding code. The average photon energy is about 1.5 MeV. The electron generation rate was estimated from the following relation:

$$\Phi_{\gamma,\,in} - \Phi_{\gamma,\,out} = \Phi_{\gamma,\,in}\,(1 - e^{-\bar{\mu}R})$$

where (see Figure 8):

$\Phi_{\gamma,\,in}$ = Gamma flux incident on a square centimeter of a beryllium shell, photons/cm^2 - sec

$\Phi_{\gamma,\,out}$ = Gamma flux transmitted through a square centimeter of a beryllium shell, photons/cm^2 - sec

$\bar{\mu}$ = Linear gamma ray mass absorption coefficient for beryllium, cm^{-1}

R = Range of the electrons in beryllium for an average electron energy of 0.75 MeV

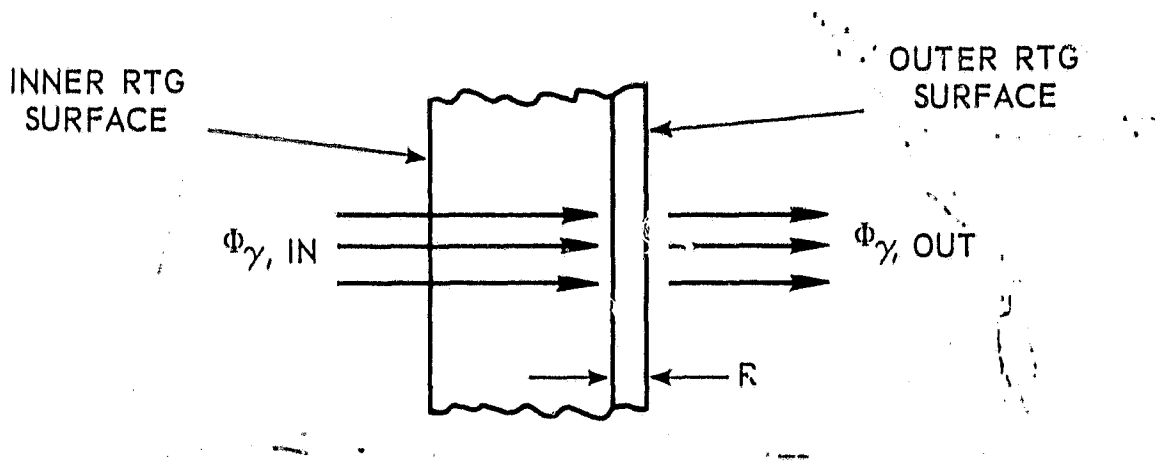

Figure 8. Electron Emission Model

*Spacecraft has 2 RTG's each fueled with PuO_2 isotope of approximately 1725 watts (thermal).

For an incident gamma flux of 2.5×10^5 photons/cm^2 - sec, the above equation yields:

$$\Phi_{\gamma,\,in} - \Phi_{\gamma,\,out} = 2.4 \times 10^3 \text{ photons/cm}^2 - \text{sec}$$

This represents the number of photons which were involved in Compton scatters within one square centimeter and R cm. deep. Thus, it is equivalent to an electron generation rate. The probability that the electrons will escape the beryllium is measured by the electron transmission coefficient. The coefficient is about 0.45, based on data in Reference 19. Thus, we have that about $2.4 \times 10^3 \times 0.45$, or 1.1×10^3 electrons/cm^2 - sec manage to escape the RTG. If the surface area of the RTG is taken as 5×10^3 cm^2, then, the electron emission rate is 5.5×10^6 electrons/sec. Since there are two 75 watt(e) RTG's involved, the total emission rate is of the order of 10^7 electrons/sec. This represents an upper limit since the charge cancellation due to internally generated electrons impinging on the inner surfaces of the RTG was not included. It is not inconceivable that the higher internal gamma fluxes could generate a significant number of electrons which would be available for charge cancellation. Analytic evaluation of the electron generation within the RTG would be rather involved and was not attempted in this calculation.

This number, 10^7 electrons per second, which is equivalent to a spacecraft current density of approximately 1.2×10^{-13} amp/meter^2,* is insignificant compared with the number of electrons produced by photoemission (see Tables 4 and 5), for example, and will therefore have no appreciable effect on spacecraft potential up to the vicinity of Jupiter, and to a distance of 10 AU.

Neutron-induced charged particles are expected to be of second order effect and are not included in this analysis.

* $\dfrac{\text{Flux, electrons/sec} \times \text{electron charge}}{\text{Assumed Surface Area of spacecraft, meter}^2} = \dfrac{10^7 \times 1.6 \times 10^{-19}}{4\pi(1)^2} = 1.2 \times 10^{-13} \dfrac{\text{amp}}{\text{meter}^2}$

SECTION III

CURRENT DENSITY FROM VARIOUS SOURCES

To evaluate the relative importance of the various sources of charge build-up, the current densities typical of each source have been calculated. In Earth's magnetosphere these densities are directly related to the omnidirectional flux plotted in Figure 5. The current in amperes per square meter is simply 1.6×10^{-19} (the electronic charge) times the flux. The anticipated value of the photo-electric current density i_{ph} is also shown in Figure 5.

Current density scales are provided in a similar manner in Figures 6 and 7, which show the variation in high-energy electron and proton flux with altitude above Earth within the magnetosphere.

Current densities typical of the transition region including the Earth's magnetosheath and the adjacent interplanetary region at about 1 AU are listed in Table 4. The same Table also lists the current density from photoemission which clearly predominates over the other current sources.

Table 5 lists various current densities in the region near Jupiter from the sources discussed in detail in Paragraph II-B-3. Thermal ion current densities were calculated for two different conditions: (1) for a corotating megnetosphere

Table 4

Near-Earth Current Densities (in A/m^2) for
Magnetosheath and Interplanetary Region at 1 AU

Particle Density Range	Magnetosheath (Region 2 of Table 1)		Interplanetary Region		Photo-Electric Current Density (i_{ph})
	Electron Current Density	Ion Current Density	Electron Current Density	Ion Current Density	
Min.	3.3×10^{-6}	2.0×10^{-7}	3.4×10^{-7}	9.6×10^{-8}	
Average	8.6×10^{-6}	5.2×10^{-7}	8.9×10^{-7}	2.5×10^{-7}	4×10^{-5}
Max.	3.0×10^{-5}	1.9×10^{-6}	3.1×10^{-6}	9.6×10^{-7}	

Table 5

Near-Jupiter Current Densities (in A/m^2)

Radius R_j (Jupiter Radii)	Particle Density Range	Thermal Electrons ($\times 10^{-8}$)	Thermal Ions ($\times 10^{-8}$)		High-energy Protons ($\times 10^{-8}$)	High-energy Electrons ($\times 10^{-8}$)
			Corotating Magnetosphere	Non-rotating Magnetosphere		
8	Min. Av. Max.	17 86 440	1.6 7.9 40	0.49 2.4 13	160	0.016
9	Min. Av. Max.	10 53 270	1.5 7.0 35	0.31 1.5 7.5	160	0.032
10	Min. Av. Max.	7.1 35 180	0.80 4.0 20	0.20 1.0 5.0	32	0.03
15	Min. Av. Max.	1.4 7.1 35	0.20 1.0 5.0	0.038 0.19 0.95	—	—
20	Min. Av. Max.	0.44 2.2 11	0.17 0.85 4.3	0.012 0.059 0.29		
30	Min. Av. Max.	0.088 0.44 2.2	0.026 0.13 0.63	0.0022 0.011 0.055		
50	Min. Av. Max.	0.012 0.058 0.29	0.0052 0.026 0.13	0.00030 0.0015 0.0075		
Photoelectric current density, $i_{ph} = 150 \times 10^{-8}$ amp/m^2						

and (2) for a non-rotating magnetosphere. The current densities from the high-energy trapped electrons and protons were based on the flux data from Eggan's report (Ref. 10). As indicated previously, no modifications were made to this data to take into account the possibility of encountering trapped electrons with energies below 5 MeV.

An examination of the current-density data indicates that the predominant sources of charge build-up will apparently be the photoemission from the spacecraft and the high-energy protons trapped in the magnetic field around Jupiter. The current density from photoemission decreases rapidly with a positive spacecraft potential, whereas the thermal electron current density increases linearly with positive spacecraft potential. The importance of this is shown in the graphical calculation of floating potential, V_f that has been included later in Section IV.

SECTION IV

SPACECRAFT FLOATING POTENTIAL

When the spacecraft reaches an equilibrium or floating potential in space, the current emitted from the spacecraft is balanced by the flow of arriving charged particles. Calculations of this potential are based on analytical expressions published by several investigators (Refs. 11, 13, and 15) concerned with the problem of determining the floating potential of a spherical body in a plasma. In such calculations the complex configuration of the spacecraft can be represented by a sphere without introducing significant errors. Other geometric models could have been assumed but because of the Debye length it is believed that a sphere is the more accurate. Local effects, such as exposed terminals of a power source (RTG), while not treated here, require special attention for a detailed design of a spacecraft. Whipple (Ref. 13) has given a comprehensive study of the equilibrium floating potential of a spacecraft together with solutions in the space environment near Earth.

A. CHARGE POTENTIAL EQUATIONS

For a stationary conductor in a plasma, the floating potential is simply given by (Ref. 16):

$$V_f = \frac{kT_e}{2e} \ln\left(\frac{\pi m}{M}\right) \tag{6}$$

where:

V_f is the floating potential,

k is Boltzmann's constant,

T_e is the electron temperature, in °K,

e is the electron charge,

m is the electron mass, and

M is the ion mass.

In a plasma with a Maxwellian distribution for the electrons at infinity, the electron current to a sphere at potential ϕ (when ϕ is negative) is:

$$I_e = -\pi r^2 A e n \left(\frac{2kT}{\pi m}\right)^{1/2} \exp\left[\frac{e\phi}{kT_e}\right] \qquad (7)$$

where:

r is the radius of the sphere,

n is the electron (and ion) density, and

A is a factor such that $1 \leq A \leq 2$, to take into account the restriction on electron collection in a magnetic field (Ref. 13); the factor A is further decreased by the reduction of electron collection in the wake of a supersonic body.

The ram ion current due to motion of the spacecraft, neglecting thermal motion, is given in Equation (8) (Ref. 13, p. 28)

$$I_i = \pi r^2 e n V_o \left[1 - \frac{2e\phi}{MV_o^2}\right], \qquad (8)$$

where V_o is the spacecraft velocity.

Sagalyn et al. (Ref. 21) derived a formula for the ion current including the effect of thermal motion that can be approximated by the expression

$$I_i = \pi r^2 n e \left(\frac{8kT_i}{\pi M} + V_o^2\right)^{1/2}, \qquad (9)$$

Equations (8) and (9) are combined by substituting

$$\left\{\left[(8kT_i)/(\pi M)\right] + V_o^2\right\}^{1/2}$$

for V_o in Equation (8) to give;

$$I_i = \pi r^2 n e \left(\frac{8kT_i}{\pi M} + V_o^2\right)^{1/2} \left[1 + \frac{2eV}{M\left(\frac{8kT_i}{\pi M} + V_o^2\right)}\right] \quad (10)$$

When equilibrium is reached, the electron current will presumably just balance the ion current at a particular value of potential V that is called the floating potential, V_f. The electron current given by Equation (7) can, therefore, be equated to the ion current given by Equation (10). However, the current resulting from photoemission must also be added to the ion current. If the electron current to the sphere predominates so that the floating potential is negative, then all the electrons generated by the photoelectric effect will escape and this part of the total current will be independent of the potential.

For the negatively charged sphere, therefore, equating (7) with (10) and including the photoelectric current gives the following expression for the floating potential, V_f:

$$V_f = -\frac{kT_e}{e}\left\{\frac{1}{2}\ln 2A^2\frac{kT_e}{\pi m} - \ln\left[\left(\frac{8kT_i}{\pi M} + V_o^2\right)^{1/2}\left(1 - \frac{eV_f}{E_i}\right) + \frac{i_{ph}}{ne}\right]\right\} \quad (11)$$

where E_i is the ion energy

$$\frac{M}{2}\left(\frac{8kT_i}{\pi M} + V_o^2\right),$$

and i_{ph} is the photoelectric current density.

Since this equation does not give an explicit solution for V_f, and iterative procedure is necessary, which has been implemented by a computer program.

If the sphere is charged positively because the ion and photoelectron currents are predominant, then the solution for the floating potential takes a different form. The expression for the thermal electron current becomes

$$I_e = -\pi r^2 A n e \left(\frac{2kT_e}{\pi m}\right)^{1/2}\left(1 + \frac{e\phi}{kT_e}\right). \quad (12)$$

The ion current is given by Equation (10) and the photoelectric current is approximated by

$$I_{ph} = \pi r^2 \, i_{ph} \, e \, \exp\left(\frac{-e\phi}{k T_{ph}}\right), \tag{13}$$

where T_{ph} is taken as 1 eV.

Then the floating potential is given by

$$V_f = -\ln\left[V_f\left(\frac{1.41\,Ae}{(\pi m k T_e)^{1/2}} + \frac{2e}{M\left(\frac{8kT_i}{\pi M} + V_o^2\right)}\right) - \left(\frac{8kT_i}{\pi M} + V_o^2\right)^{1/2} + A\left(\frac{2kT_e}{\pi m}\right)^{1/2}\right] + \ln\frac{i_{ph}}{ne} \tag{14}$$

Again, the term V_f appears in both sides of the equation so that an iterative procedure based on a computer program becomes necessary to obtain a solution in a reasonable length of time.

B. SPACECRAFT POTENTIAL

This section combines the considerations and equations developed in Section IV, A, together with the environmental parameters in Section II to give the floating potential of a spacecraft in the various environments encountered on the NEW MOONS mission.

The equilibrium floating potential, calculated from Equations (11) or (14) for a spherical body in the magnetosphere, is shown in Figure 9.

For the Earth's magnetosheath region and interplanetary space, the floating potential is given in Table 6, for the conditions in Table 4. The floating potential in interplanetary space will not vary if the density varies as $1/r_s^2$ and the velocity and temperature remain constant.

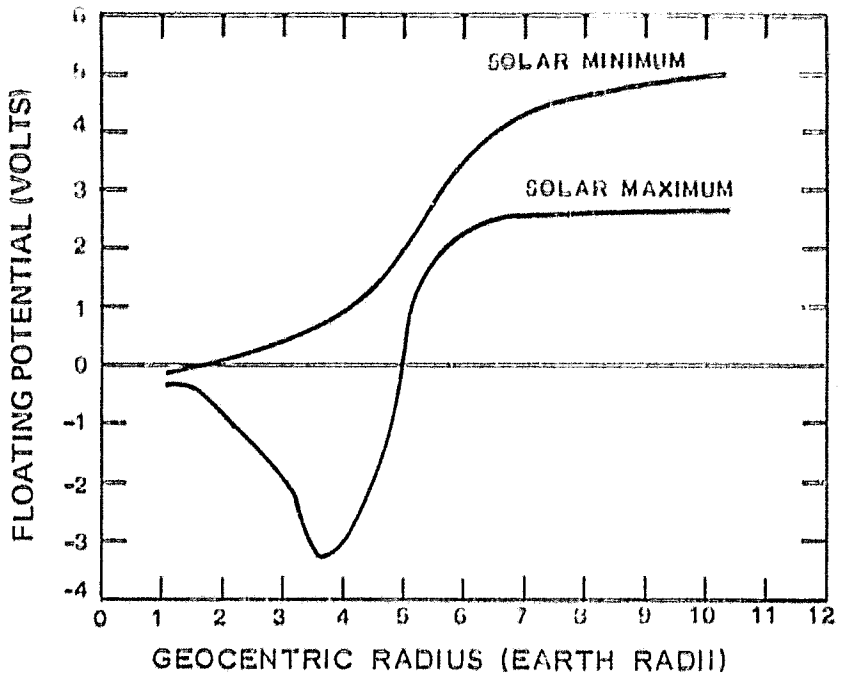

Figure 9. Equilibrium Floating Potential in the Magnetosphere

Table 6

Spacecraft Floating Potential (Volts)
for the Earth's Magnetosheath Region and Interplanetary Space

Particle Density Range	Magnetosheath (Region 2, Table 1)	Interplanetary Space (Regions 3 and 5, Table 1)
Minimum	2.4	4.0
Average	1.6	3.4
Maximum	0.9	2.6

For the Jupiter environment model the floating potential is given in Table 7. Column A gives the results of calculations from Equations (11) or (14) for a corotating magnetosphere (i.e. $V_o = \Omega R_j + V_o'$). Column B gives the results of calculations for a stationary magnetosphere and column C is an approximate solution with the high energy proton and secondary emission currents included.

The equilibrium floating potential for this last case can be determined in a relatively simple manner by a graphical procedure. The individual components of the charging current as a function of spacecraft potential are plotted separately

Table 7

Spacecraft Floating Potential for Near-Jupiter Environment

Radius R_j (Jupiter Radii)	Condition Range	Co-rotating Magneto-Sphere	Stationary Magneto-Sphere	Approximate Solution*
		A	B	C
8	Min. Av. Max.	1.9 0.55 -3.6	1.9 0.48 -4.1	81 16 1.6
9	Min. Av. Max.	2.3 0.95 -1.6	2.2 0.87 -2.2	129 26 4.0
10	Min. Av. Max.	2.7 1.3 -0.10	2.6 1.2 -0.57	80 9.6 2.4
15	Min. Av. Max.	4.1 2.7 1.3	4.0 2.6 1.2	
20	Min. Av. Max.	5.1 3.7 2.3	5.0 3.6 2.2	
30	Min. Av. Max.	6.7 5.2 3.7	6.5 5.1 3.6	
50	Min. Av. Max.	8.6 7.1 5.6	8.3 6.9 5.5	

*Includes high-energy proton and secondary-emission currents based on Jupiter model of Reference 10.

on the same graph. Curves representing the total positive or negative current are obtained by adding the appropriate positive or negative components. The coordinates of the intersection of the total positive and negative current curves, where the two currents are equal, give the equilibrium potential and the currents to the spacecraft. This procedure is illustrated in Figure 10 for a particular set of conditions. The negative current sources are thermal electrons and high energy electrons. The positive current includes the contributions from thermal protons, high energy protons, secondary electrons generated by the bombarding protons and from photoemission. In calculating the secondary emission current, it was assumed that a secondary emission coefficient for ion bombardment was 2, corresponding to materials normally forming the outer surface of the spacecraft, and the emitted electrons have a Maxwell distribution with an equivalent temperature of 3.8 eV. The intersection of the positive and negative current indicates that the floating potential will be about 15 volts.

Although the equations for charge collection and floating potential are approximate, and the complex shape of the baseline GJP spacecraft is approximated by a sphere, it is felt that the calculations are reasonably accurate and indicate the importance of the various sources of charge. The effects of the magnetic field are taken into account in regions near the Earth and near Jupiter where the electron gyro-radius becomes comparable to or less than the spacecraft dimensions. In Equations 11 and 14, the factor "A" is varied appropriately.

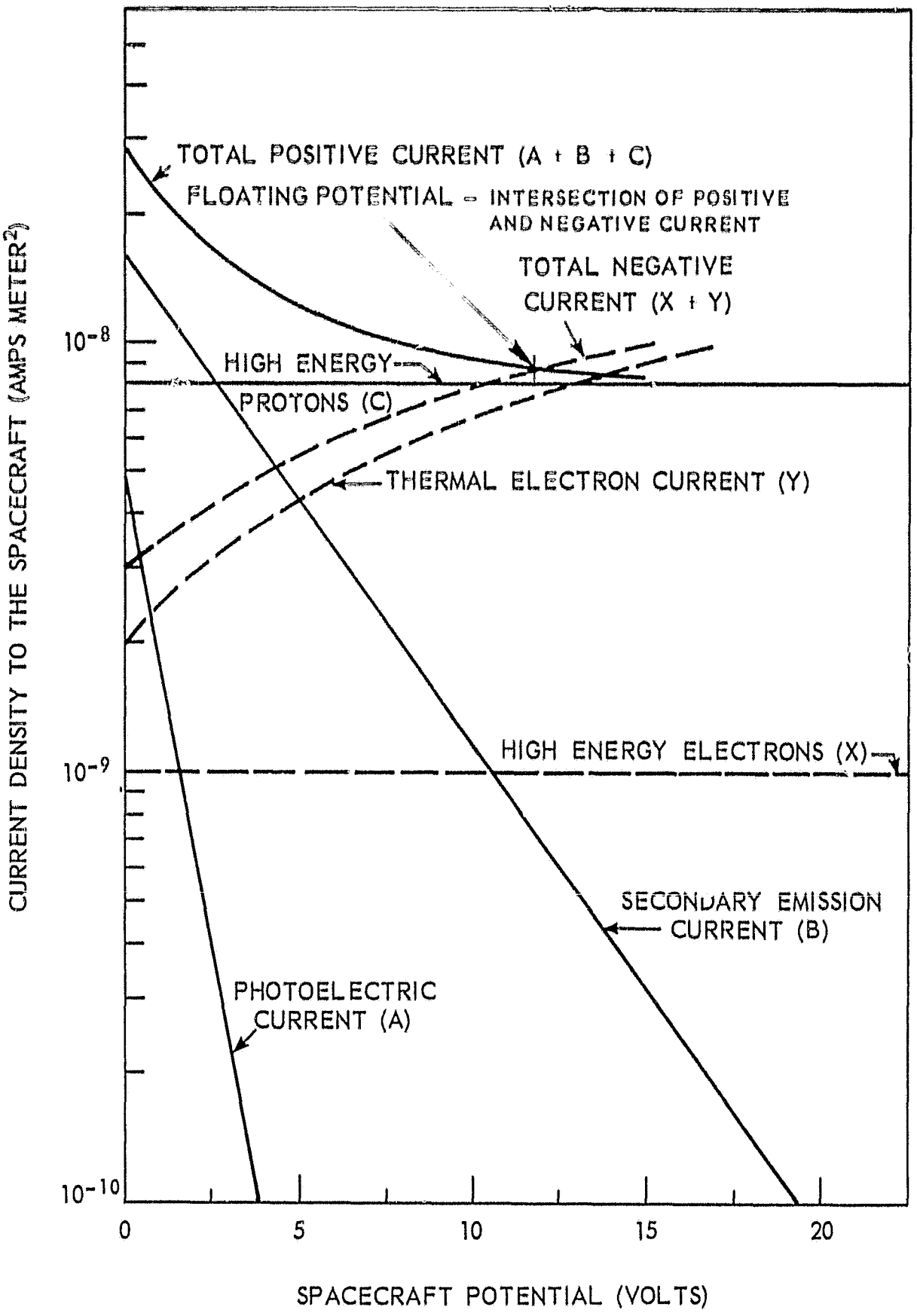

Figure 10. Graphical Method to Determine the Floating Potential of a Spacecraft in the Presence of High Energy Radiation – Sample Calculation at Jupiter

Note: Spacecraft potential is independent of spacecraft size within the range of the model selected

SECTION V

PROTECTIVE MEASURES RECOMMENDED FOR CHARGE BUILD-UP PROBLEM AREAS

The assumption that the photoelectron spectrum was Maxwellian is only approximately valid. There is a high-energy tail on the energy distribution so that if the ambient density and electron temperatures are sufficiently low the higher energy photoelectrons could result in a larger positive potential. In laboratory measurements of the photoemission from aluminum it was found that i_{ph} was an order of magnitude larger than tungsten. However, in experiments with rockets flights, the photoemission from aluminum was found to be of the same order as tungsten and approximately the value used (Ref. 11). This is probably due to oxidation of the surface. As the photoelectric density is large in most environments, consideration should be given to reducing the total photoelectric current. For example, if the radio dish antenna were made of mesh rather than a solid material, the photoelectric current would be significantly reduced and the thermal electron collection would be increased. Materials with a high photoelectron yield should be avoided on the sunward side of the spacecraft.

The flux of high energy protons in Jupiter's outer radiation belt is a possible problem area based upon Eggan's figures and if the thermal electron flux is low. However, the energy spectra of the protons and electrons in the Jovian magnetosphere is likely to be similar to that encountered in the Earth's magnetosphere and consequently there will be a large flux of electrons and protons in the energy range from 200 eV to 40 KeV throughout the magnetosphere. This will tend to dominate over the flux of very high energy protons and to lower the floating potential to a few volts. This is one area that should be investigated more thoroughly.

A vehicle with very long booms moving across a magnetic field will develop an electric field along the booms equal to $\vec{V} \times \vec{B}$, where $\vec{V}$ is the vehicle velocity, and $\vec{B}$ is the magnetic field. If the magnetosphere of Jupiter is corotating with the planet, the maximum relative velocity would be 131 km/sec and the magnetic field is 2.2×10^{-6} Teslas, giving an electric field of 0.29 volts/meter. The potential across the GJP booms, if the booms are oriented perpendicular to the magnetic field, would be about 1.0 volts. The problem of $\vec{V} \times \vec{B}$ potentials and sheaths has been discussed by Osborne and Kasha (Ref. 17) in relation to the Alouette satellites.

In a discussion of the problems associated with charge collection and vehicle potential, it is necessary to consider the types of experiments that will be affected and what the effects will be. Such spacecraft functions as communication

will not be affected by either charge collection or spacecraft potential and, of course, neither optical nor radio experiments will be affected.

Experiments for measuring high-energy particles (i.e., particle energy (eV) >> spacecraft potential) will be affected very little by the potential. In experiments to measure, directly, the flux or energy of thermal ions or electrons such as Langmuir probes or Faraday-cup probes, the results will be strongly affected by the charge collection and emission, the spacecraft potential, and the sheaths surrounding the spacecraft. Experiments of this type often use the spacecraft potential as a reference, in which case it is necessary to provide the instruments with a large enough dynamic voltage range that the sensors may be swept through the plasma potential, several times (kT_e/e) volts positive and negative. The emission of secondary and photoelectrons from the spacecraft creates an electron sheath around the spacecraft (Ref. 18), and probes measuring the thermal electrons would detect these secondary and photoelectrons. The problem of sheaths around a moving spacecraft is very complex and the interpretation of low-energy sensors in these sheaths is even more so; for example see Reference 18. Resonance r-f probes are also sensitive to the characteristics of the sheath.

SECTION VI

CONCLUSIONS

In the several environments to be encountered by the spacecraft on the NEW MOONS mission considered for this Task, the radiation from the RTG's and the associated secondary radiation will not be a major source of charging for the spacecraft. In the environments that have been considered, the spacecraft generally will come to an equilibrium potential a few volts positive with respect to the ambient plasma potential. A possible problem area would be in the high-energy proton radiation belts of Jupiter if the proton flux is high, as in Eggan's model, with an accompanying low flux of thermal electrons.

The effects of a positive floating potential on experiments have been considered. Where the energy range of the particles being measured is much greater than the spacecraft potential, the potential will have little effect on the measurements. The measurement of thermal particles is strongly affected by the spacecraft potential, the charge collection and emission, and the sheath. It is therefore necessary to consider all these phenomena in interpreting the data.

LIST OF REFERENCES

1. R. Gendrin, "Progress Recents dans l'Elude des Ondes T.B.F. et E.B.F.", Space Science Rev., Vol. 7, pp. 314-395 (1967).

2. G. W. Haydon and D. L. Lucas, "Predicting Ionosphere Electron Density Profiles", Radio Science, Vol. 3, p. 111-119 (1968).

3. Ja. L. Al'pert, "On the Outer Ionosphere (and the Transition into Interplanetary Space)", Space Sci. Rev., Vol. 6, pp. 419-451 (1967).

4. G. P. Serbu and E. J. R. Maier, "Low Energy Electrons Measured on Imp. 2", Jour. Geophys. Res., Vol. 71, pp. 3755-3766 (1966).

5. Significant Achievements in Space Science, 1966, NASA SP-155.

6. L. A. Frank, "Several Observations of Low Energy Protons and Electrons in the Earth's Magnetosphere with OGO 3", Jour. Geophys. Res., Vol. 72, pp. 1905-1916 (1967).

7. J. R. Spreiter, A. L. Summers, and A. Y. Alksne, "Hydromagnetic Flow Around the Magnetosphere", Planet. Space Sci., Vol. 14, pp. 222-253 (1966).

8. J. A. Roberts, "Jupiter, as Observed at Short Radio Wavelengths", Symposium on Planetary Atmospheres and Surfaces, Radio Science, Vol. 69D, pp. 1543-1552 (1967).

9. G. R. Ellis, "The Decametric Radio Emission of Jupiter", Radio Science, Vol. 69D, pp. 1513-1530 (1967).

10. J. B. Eggan, "The Trapped Radiation Zones of Jupiter", General Dynamics Report FZM-4789, Gen. Dyn. Fort Worth Div. (1967).

11. U. Fahleson, "Theory of Electric Field Measurements Conducted in the Magnetosphere with Electric Probes", Space Sci. Res., Vol. 7, pp. 238-262, (1968).

12. H. E. Hinteregger and K. R. Damon, "Analysis of Photoelectrons from Solar Extreme Ultraviolet", Jour. Geophys. Res., Vol. 64, No. 8, pp. 961-969 (1959).

13. E. C. Whipple, Jr., "The Equilibrium Electric Potential of a Body in the Upper Atmosphere and In Interplanetary Space", NASA Report X-615-65-296, June 6, 1965.

14. R. S. White, "Time Dependence of Low Energy Proton Belts", Jour. Geophys. Res., Vol. 72, pp. 943-950 (1967).

15. U. Samir, A. P. Willmore, "The Equilibrium Potential of a Spacecraft in the Ionosphere", Planet. Space Sci., Vol. 14, pp. 1131-1137, (1966).

16. F. F. Chen, "Plasma Diagnostic Techniques", Chapter 4, p. 177, R. H. Huddlestone and S. L. Leonard, Ed., Academic Press (1965).

17. F. J. F. Osborne and M. A. Kasha, "The V × B Interaction of a Satellite with its Environment", Can. Jour. Phys., Vol. 45, pp. 263-277 (1967).

18. D. B. Medev, "On the Formation of Satellite Electron Sheaths Resulting from Secondary Emission and Photoeffects", Interactions of Space Vehicles with an Ionized Atmosphere, ed. S. F. Singer, Pergamon Press, p. 305, (1965).

19. C. D. Magnuson and A. W. McReynolds, "Space Electron Radiation Shielding - Bremsstrahlung and Electron Transmission", 2nd Sympos. on Protection Against Radiation in Space, NASA, Wash., p. 455 (1965).

20. D. B. Melrose, "Rotational Effects on the Distribution of Thermal Plasma in the Magnetosphere of Jupiter," Planetary and Space Science, p. 381, (1967).

21. R. C. Sagalyn, M. Smiddy, and J. Wisnia, "Measurements and Interpretation of Ion Density Distribution in the Daytime F Region," Jour. of Phys. Research, Vol. 68, p. 199, (1963).